Interactive Mesh Generation with Local Deformations in Multiresolution

Renan Dembogurski[1]*, Bruno Dembogurski[2], Rodrigo Luis de Souza da Silva[1], and Marcelo Bernardes Vieira[1]

[1] Department of Computer Science, Universidade Federal de Juiz de Fora (UFJF)
DCC/ICE, R. Lourenço Kelmer, 36036-330, Juiz de Fora, MG, Brazil
[2] Computer Institute - IC, Universidade Federal Fluminense (UFF) - IC/UFF
Rua Passo da Pátria 156 - Bloco E, 24210-240, Niterói, RJ, Brazil
{renan.augusto,rodrigoluis,marcelo.bernardes}@ice.ufjf.br
{bdembogurski}@ic.uff.br

Abstract. This work presents a method to model a spherical mesh by modifying its heightmap in an augmented reality environment. Our contribution is the use of the hierarchical structure of semiregular A4-8 meshes to represent a dynamic deformable mesh suitable for modeling. It defines only a fraction of the overall terrain that is subjected to local deformations. The modeling of spherical terrains is achieved with proper subdivision constraints at the singularities of the parametric space. An error metric dependent on the observer and on the geometry of the topography was used to provide fast visualization and editing. The results demonstrate that the use of the A4-8 mesh combined with the tangible augmented reality system is flexible to shape spherical terrains and can be easily modified to deal with other topologies, such as the torus and the cylinder.

Keywords: Mesh Deformation, 4-8 Semi-regular Adaptive Meshes, Augmented Reality.

1 Introduction

Mesh deformation is an important resource for the object modeling area, allowing the modification of a surface to suit a particular purpose. Due to its importance, several deformation techniques have been developed, as seen in [1], [2] and [3], where some of these take into account the decomposition of highly detailed surfaces in hierarchical levels [4], [5]. Representing a surface by multiple levels of detail allows changes to be made at any of these levels, resulting in a fine control of the mesh.

A hierarchical structure that has favorable properties for representation and modeling of a terrain at various levels of detail is a semi-regular 4-8 adaptive mesh (A4-8 mesh [6]). Through this structure, it is possible to represent terrains

* Authors thank to Fundação de Amparo à Pesquisa do Estado de Minas Gerais and CAPES for financial support.

with different resolutions, allowing punctual control over the generated mesh. The A4-8 can also define a parametric space to calculate coordinates on a $\mathbb{R}^3$ Euclidean space.

One of the possible ways to interact with 3D models is through fiducial markers in an augmented reality environment. In this scenario, real and virtual elements are combined to create the impression that they coexist in the same scene. To interact with virtual models an interface called Tangible Augmented Reality (TAR) [7] can be used, where each virtual object is associated with a physical object and the user interacts with the virtual objects by manipulating tangible objects.

This work proposes a method to deform spheric terrains through the combination of an A4-8 structure and tangible markers. Local deformations are applied to a fraction of the overall terrain, resulting in an application that allows both visualization and modification of a terrain in real time. The A4-8 hierarchical structure provides the method with a precise control over the surface to be modified.

2 Related Work

There are not many works that deal with the problem of deforming meshes through augmented reality. Also, the focus of most studies involving object modeling and augmented reality is in the deformation models in general, or the development of applications for remote areas such as surgical operations simulation [8], clothes modeling [9] and accidents modeling [10].

A work that allows interactive modification of multiresolution polygon meshes through a 3D interface can be found in [11]. The authors propose an interface called *inTouch*, which contains a projected 3D scene where the model is modified and a 2D menu for operations. The interface has a multiresolution meshes editing subsystem, which takes as input the position of the haptic device probe projected onto the scene and the direction of the applied force.

When the mesh is modified at a particular resolution, a set of vertices is moved. The change is then propagated to the higher detailed levels through mesh subdivision and to the less detailed levels through smoothing. The mesh editing subsystem receives a triangle, a contact point and a motion vector as input. In our method, the control point is a vertex and the deformation is propagated only to the resolution levels which are higher than that point.

An example of work that uses augmented reality and a tangible user interface for modeling 3D objects, can be found in [12], where a system called *3DARModeler* is presented. With this system it is possible to create a 3D model through one or several primitive geometries, apply textures, add animations, estimate real light sources and cast shadows on it. The difference between this system and the one developed in this work, with respect to modeling, is that the 3D models used by the *3DARModeler* are static. In this paper, the proposal is to dynamically change the geometry of a surface at multiple levels of detail, pro-

viding greater user interaction with the model and, also, overall control over the mesh.

3 A4-8 Meshes

Among the various categories of regular meshes, it is necessary to choose one that not only represent a terrain, but also can support simplification and refinement methods. The semi-regular meshes of type 4-8 (vertices with valence equal to 4 or 8, except at the edges) fit the desired profile to solve the problem addressed in this work. The semi-regular 4-8 mesh is a hierarchical structure for subdivision surfaces, or a complex cellular homeomorphic to a $[4, 8^2]$ Laves tiling [6].

The semi-regular 4-8 meshes can be divided into adaptive and non-adaptive. In the case of non-adaptive, there is only one hierarchy in the mesh, meaning that the modifications made in a region of the mesh affect the resolution of the entire grid. In the case of adaptive ones, there is a family of hierarchies, so that there is no interference between local modifications at each level.

This work uses adaptive meshes in order to deform a terrain at different levels of detail, independent of each other, and view it in different resolutions through simplifications or refinements. An example of this structure can be seen in Figure 1, where it is shown a basic block of the structure and two steps of consecutive refinement over it.

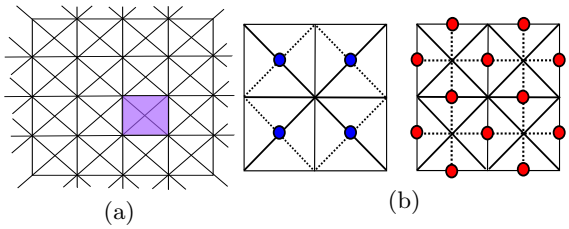

Fig. 1. Structure of a 4-8 mesh, (a) shows the basic construction block in purple and (b) shows two steps of refinement, the first generates the vertices in blue and the second, the vertices in red

An A4-8 mesh can be constructed using two approaches: top-down and bottom-up. The top-down approach, also known as refinement method, characterizes itself for creating a mesh in the lowest possible resolution and, progressively, increasing the resolution through the creation and addition of new triangles to the mesh. The bottom-up approach, or simplification method, creates a mesh in the highest possible resolution and, in a similar way, reduces the resolution by uniting the mesh triangles.

In this work, the mesh is constructed using a strictly top-down approach in the tessellation process. This way, it is possible for the final application to maintain its efficiency even with modifications being done to the mesh in real time.

3.1 Triangle *Bintree*

This work uses the binary triangle tree structure, or triangle *bintree* [13], to represent a terrain. Consider an A4-8 mesh M with a set of vertices $\mathbf{V} \subset \mathbb{R}^2$ given by $\mathbf{V} := \{\vec{v_i} := (u_i, v_i) \in \mathbb{R}^2, i = 1, ..., n\}$, where n is the number of vertices. A triangle bintree is a binary tree where, geometrically, every node of the tree represents a triangle.

The root triangle, $T = (\vec{v_a}, \vec{v_0}, \vec{v_1})$ where $\vec{v_a}, \vec{v_0}, \vec{v_1} \in \mathbf{V}$, is define as a right isosceles triangle in the coarser level, ($l = 0$). In the next level, $l = 1$, the children of the root are defined through the insertion of an edge defined between the apex vertex $\vec{v_a}$ and the middle point $\vec{v_c} \in \mathbf{V}$ of the base edge $(\vec{v_0}, \vec{v_1})$. The left children is $T_0 = (\vec{v_c}, \vec{v_a}, \vec{v_0})$ and the right children is $T_1 = (\vec{v_c}, \vec{v_1}, \vec{v_a})$. Repeating this process recursively, the rest of the tree is obtained. Figure 2 shows a few levels of a triangle bintree.

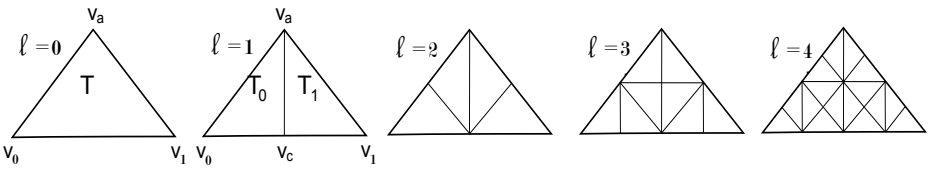

Fig. 2. Levels 0−4 of a triangle bintree.

It is important to note that the described structure needs to be adapted in a way that the A4-8 mesh can represent a spherical terrain. When subdividing a triangle at the first or last meridian, a middle point vertex must be created for both meridians. These vertices are "connected", meaning that any modification done to one of them must be applied to the other in order to prevent cracks on the mesh. This procedure ensures that the plane is conformed according to the cylinder topology.

Another important factor to be mentioned is that, for each vertex $\vec{v} \in \mathbf{V}$, two values must be stored, w e ε. The first value, w, represents the height of a vertex defined as $w = g(f(u, v)) = g(x, y, z)$, where f is a mapping function $f : \mathbb{R}^2 \to \mathbb{R}^3$ and g is a function that uses the mapped vertex coordinates, x, y and z, to calculate a height value. The resulting scalar is stored in a scalar matrix (heightmap M_a) at the vertex $\vec{v}$ coordinates u and v.

The second value, ε, represents the error value of each vertex $\vec{v} \in \mathbf{V}$. This value will be detailed in Section 5.1. In a resumed way, the vertex error is defined as $\varepsilon = \varepsilon_T$, where ε_T is the triangle error that has $\vec{v}$ as apex vertex. In practice, a triangle error value ε_T, for $T = (\vec{v_a}, \vec{v_0}, \vec{v_1})$, is stored in a scalar matrix (error map M_e) at the triangle T apex vertex $\vec{v_a}$ coordinates, u and v.

4 Parametrization

A parametric surface in the Euclidean space $\mathbb{R}^3$ is defined by a parametric equation with two parameters, named in this work as u and v. In particular, we want a mapping $f : \Omega \rightarrow \mathbf{S}$, where f is a mapping function, Ω is an open subset $\Omega \subset \mathbb{R}^2$ and $\mathbf{S}$ is a surface $\mathbf{S} \in \mathbb{R}^3$.

Orthographic projection was used as a function f to map Ω in S. More specifically, a plane, represented by A4-8 mesh, in a sphere. Consider, the vertex set $\mathbf{V}$ of a A4-8 mesh is Ω and all vertices $\vec{v} \in \mathbf{V}$ are associated with coordinates u and v in the plane. Consider also, that $0 \leq u \leq m_u$ and $0 \leq v \leq m_v$.

To define a function f in terms of latitude and longitude of a vertex $\vec{v} \in \mathbf{V}$, it is necessary to calculate the latitude of $\vec{v}$ using Equation 1 and its longitude using Equation 2.

$$latitude = \frac{(v * \pi)}{m_v} - \frac{\pi}{2}. \tag{1}$$

$$longitude = \frac{(2u * \pi)}{m_u} - \pi. \tag{2}$$

Now consider that the radius of the sphere defined by $\mathbf{S}$ is r. The domain surface V and S can be written using Equations 3 and 4, respectively.

$$\mathbf{V} = \{(u, v) \in \mathbb{R}^2 : 0 \leq u \leq m_u, 0 \leq v \leq m_v\}. \tag{3}$$

$$\mathbf{S} = \{(x, y, z) \in \mathbb{R}^3 : x^2 + y^2 + z^2 = r^2\}. \tag{4}$$

A plane to sphere mapping function is defined in Equation 5.

$$f(u, v) = \begin{pmatrix} r * \cos(longitude) * \cos(latitude), \\ r * \sin(longitude) * \cos(latitude), \\ r * \sin(latitude) \end{pmatrix}. \tag{5}$$

From this point on in this work, $\vec{v}$ will be used as a notation for describing a vertex that belongs to $\mathbf{V}$, which is a vertex of the mesh in discrete domain. To differentiate, $\vec{\mathbf{v}}$ will be used when the vertex is in continuous domain, in other words, the vertex mapped by $f(u, v)$ which has coordinates x, y and z.

When the set of vertices to be deformed is defined, the values of height are calculated in the continuous domain for each one of these vertices. The calculation is done through a function g and the values obtained are stored in the heightmap. This way, the terrain deformation is the modification made to the values of height w of the vertices inside a deformation area, in the discrete domain.

4.1 Parameter Space Partitioning

To obtain a partition $\mathbf{N} \subset \mathbf{V}$ endowed with all vertices $\vec{v}$ that when mapped to $\mathbb{R}^3$ are within a certain distance of a control vertex $\vec{\mathbf{v_c}} \in \mathbb{R}^3$, it is necessary to discretize the continuous object that represents the area of deformation in $\mathbb{R}^3$. More specifically, it is desired to obtain a partition of $\mathbf{V}$ having all the vertices $\vec{v}$ that, when mapped by $f(u, v)$, reside within a certain distance from a control vertex $\vec{\mathbf{v_c}} \in \mathbb{R}^3$. In other words, a partition that has all vertices $\vec{v} \in \mathbf{V}$ that reside in a deformation area defined in Euclidean $\mathbb{R}^3$ space.

To obtain $\mathbf{N}$, the Euclidean distance d in $\mathbb{R}^3$ between the vertices $\vec{\mathbf{v}}^T = [x, y, z]^T$ and the control vertex $\vec{\mathbf{v_c}}^T = [x_c, y_c, z_c]^T$ is initially calculated for all vertices $\vec{v} \in \mathbf{V}$. Then, a function is defined to classify the vertices $\vec{v_i}$ as

$$I(u, v) = \begin{cases} 1, \text{ if } d \leq r_d \\ 0, \text{ otherwise} \end{cases}, \tag{6}$$

where $I(u, v)$ is a function that uses the coordinates u and v of a vertex $\vec{v}$ to indicate if it is inside or outside of a deformation area. The value r_d is defined dynamically by the user.

This classification of the vertex according to the I function will be called property $I(u, v)$. If the function returns one, the vertex has the property, otherwise, it has not. If the vertex has the property $I(u, v)$, it is placed in the set of vertices that are inside the deformation area. This set of vertices will be called $\mathbf{V}_d$.

It's Important to note that the set $\mathbf{V}_d$ is defined in the discrete domain, but the distance is calculated in the continuous domain. This happens because, if the distance was calculated in the discrete domain, the resulting deformation area would be distorted by the mapping according to its location on the sphere.

5 Error Metric

This work uses the error metric presented by [13] in their algorithm named Real-time Optimally Adapting Meshes (ROAM). To decide if a triangle must be refined or simplified, the ROAM algorithm uses the concept of nested spaces. Being $\mathbf{C}$ the descendants of a vertex $\vec{v_i} \in \mathbf{V}$, the error $\varepsilon_{\vec{v_i}} \geq e_{\vec{v_j}}, \forall j \in \mathbf{C}$. This means that the error metric guarantees the monotonicity of the error values, in other words, the "parents" in a coarser level always have a higher error than their children, that reside in finer levels of the terrain. To use this error metric, the geometric error and the view-dependent error must be calculated for each triangle of the mesh.

5.1 Geometric Error

The ROAM algorithm uses the concept of a *wedgie* to define the geometric error. Consider that T is a triangle of the triangle bintree and the same notation of neighborhood from Section 3.1 will be used. A *wedgie* is defined as the world

volume that has the vertices (u, v, w), in a way that $(u, v) \in T$ and $|w - w_T(\vec{v})| \leq e_T$, for a certain *wedgie* thickness $\varepsilon_T \geq 0$. The line segment from $(u, v, w - e_T)$ to $(u, v, w + e_T)$ is called thickness of a segment for a vertex $\vec{v}$.

The nested errors of the *wedgies* are calculated in a bottom-up manner. It is assumed that $\varepsilon_T = 0$ for all triangles in the finest possible level. The *wedgie* thickness of a triangle T is calculated based on the *wedgie* thickness of its children, ε_{T_0} and ε_{T_1}. Consider a triangle T with a left neighbor T_0 and right neighbor T_1. The error ε_T can be calculated as

$$\varepsilon_T = max(\varepsilon_{T_0}, \varepsilon_{T_1}) + |w(\vec{v_c}) - w_T(\vec{v_c})|,$$

where $\vec{v_c}$ is the vertex obtained from the bisection of the edge opposite to the apex vertex in the triangle T and $w_T(\vec{v_c})$ is given by

$$w_T(\vec{v_c}) = \frac{(w(\vec{v_0}) + w(\vec{v_1}))}{2}.$$

5.2 View-dependent Error

The view-dependent error, called geometric screen distortion, is simply the calculation of the geometric distortion. This calculation represents the distance between the position where each vertex of the surface $\mathbf{S}$ should be in the screen space and where the triangulation touches the screen.

Be $s(\vec{\mathbf{v}})$ the correct position in screen space of a vertex $\vec{\mathbf{v}}$ given by $f(u_{\vec{v}}, v_{\vec{v}})$ and $s_T(\vec{\mathbf{v}})$ its approximation by the triangulation T. The error in this point is defined as:

$$dist(\vec{\mathbf{v}}) = \|s(\vec{\mathbf{v}}) - s_T(\vec{\mathbf{v}})\|$$

In the entire image, the maximum error is given by $dist_{max} = max_{\vec{v} \in \mathbf{V}_f}(dist(\vec{\mathbf{v}}))$, where $\mathbf{V}_f$ is the set of vertices $\vec{v}$ of the mesh that, when mapped to the sphere, reside in the view frustum (region in space that appear on the screen).

In practice, a superior limit is calculated for the maximum distortion. For each triangle T in the triangulation, a local limit is calculated, projecting the *wedgie* in the screen space. This limit is defined as the higher thickness size ε_T of all vertices $\vec{v} \in T$ projected to the screen.

6 Proposed Method

In order to deform a terrain through the modification of its height map, a method is proposed with the following steps: Definition of the control point, definition of a deformation area and propagation of heights and errors. The first stage defines where on the terrain the deformation is made. The second stage uses the control point to define a dynamic area of deformation. The last step is the most important, where error and height values are propagated to the vertices of the terrain contained within the area of deformation.

6.1 Control Point Definition

This work uses one control vertex $\vec{v_c}$, which defines the center of the propagation area of height and error values, where the proposed method starts. It is obtained during the mesh tessellation, representing the vertex of the mesh $\vec{v} \in \mathbf{V}$ that, when mapped to the sphere, is the closest one to the deformation object (predefined fiducial marker).

If the camera position approaches the area pointed by the user, it increases the model scale and the mesh goes through a refinement process that can modify the control vertex $\vec{\mathbf{v_c}}$. Likewise, if the user moves the deformation object, $\vec{\mathbf{v_c}}$ changes dynamically.

6.2 Defining the Deformation Area

The area of deformation is a set of vertices $\mathbf{V}_d \subset V$ that, when mapped to the sphere through $f(u, v)$, reside at a distance less than or equal to a radius in relation to a control point $\vec{\mathbf{v_c}} \in \mathbb{R}^3$ (Section 4.1). This value is dynamically defined by the user through the user interface and will be called, henceforth, *radius of deformation*, or r_d. The area of deformation is constructed according to a set of constraints described below.

Let $\mathbf{V}$ be the set of vertices of the A4-8 mesh. Subregions $\mathbf{V}_i \in \mathbf{V}$, representing partitions of $\mathbf{V}$ endowed with some property $I(\mathbf{V}_i)$, can be constructed by the following restrictions:

1. $\bigcup_{i=1}^{n} \mathbf{V}_i = \mathbf{V}$;
2. $\mathbf{V}_i$ is a connected region, $i = 1, 2, ..., n$;
3. $\mathbf{V}_i \bigcap \mathbf{V}_j = \emptyset \mid \forall\ i, j$ where $i \neq j$;
4. $I(\mathbf{V}_i) = 1$ for $i = 1, 2, ..., n$;
5. $I(\mathbf{V}_i \bigcup \mathbf{V}_j) = 0$ for $i \neq j$, where $\mathbf{V}_i$ and $\mathbf{V}_j$ are adjacent.

The first restriction means that the partition should be complete, in other words, all vertices of $\mathbf{V}_i$ must be contained in $\mathbf{V}$. The second requires that all vertices of the sub-region are "connected". The third constraint indicates that different subregions should be disconnected. The fourth requires that all vertices $\vec{v_i} \in \mathbf{V}_i$ must satisfy the properties $I(\mathbf{V}_i)$. The last restriction means that distinct sub-regions have different properties.

The restrictions shown above can be reinterpreted according to the problem addressed here. A property called $I(u, v)$ is defined for each vertex of the mesh according to Equation 6. This way, it is desired to partition the terrain into two disconnected sets, a set $\mathbf{V}_d$ that has vertices with the property $I(u, v)$ and another complementary to it $\bar{\mathbf{V}}_d$. Henceforth in this paper, the vertices of $\mathbf{V}_d$ will be called internal and vertices of $\bar{\mathbf{V}}_d$ will be called external.

The formulation proposed above follows the same principle of the image segmentation procedures, where usually one wants to separate the background and a region of interest. This choice is due to the fact that the almost completely regular structure of the semi-regular meshes allows the use of traditional algorithms of image processing.

6.3 Region Growing

The region growing technique was chosen as the implementation of the expansion function to define the set $\mathbf{V}_d$ ([14]). The starting point is the control vertex $\vec{v_c}$ and the expansion occurs in all of its neighbors directions while there are vertices with the property $I(u, v)$. Henceforth, the set of neighbors of $\vec{v_c}$ that have the property $I(u, v)$ will be called $\mathbf{V}_{d_c}$.

Initially, the algorithm tests the neighbors of $\vec{v_c}$ and the vertices with the property $I(u, v)$ are put in a set of vertices called $\mathbf{V}_{d_c}$. This set is passed to a recursive expansion function so the set $\mathbf{V}_d$ can be obtained. This function expands $\mathbf{V}_{d_c}$ from $\vec{v_c}$ toward the direction of each neighboring vertices $\vec{v_i} \in \mathbf{V}_{d_c}$. The neighborhood is covered in the A4-8 mesh, but the distance test is done in Euclidean space $\mathbb{R}^3$. An example of the test of a vertex $\vec{v_i}$ neighbor of $\vec{v_c}$, through the distance $\mathbf{\vec{d_{ic}}}$ between them, can be seen in Figure 3(a). The final set of vertices $\mathbf{V}_{d_c}$ can be seen in Figure 3(b).

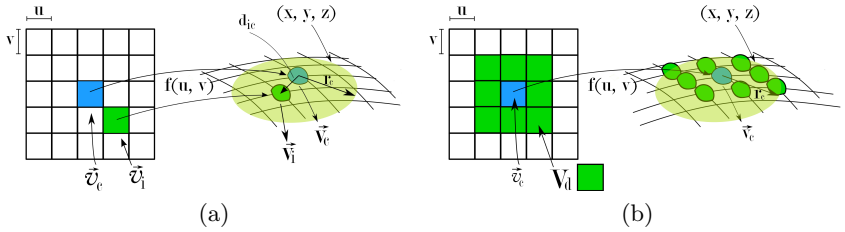

Fig. 3. (a) Beginning of the expansion process. The control vertex is $\vec{v_c}$ in the discrete domain and $\mathbf{\vec{v_c}}$ in continuous domain. The radius that defines the area of deformation is r_d and $\mathbf{\vec{d_{ic}}}$ is the distance in $\mathbb{R}^3$ between the control vertex $\vec{v_c}$ and of its neighbors $\vec{v_i}$. (b) The set $\mathbf{V}_{d_c}$, in green, represents the vertices that have the property $I(u, v)$.

The recursive function is responsible for "walking" across the mesh in the direction of each of the neighbors of $\vec{v_c}$. It is possible to separate the eight neighborhoods of a vertex in two cases, diagonal direction and vertical/horizontal direction. A neighbor is in a diagonal direction if both coordinates of the original vertex in the parameter space, u and v, change in one step of the algorithm in that direction. For the vertical/horizontal direction, one step of the algorithm modifies only one coordinate, u or v, of the original vertex.

The combination of these two cases mentioned above allows the algorithm to go through the entire deformation area over the mesh. If the direction is diagonal, the recursion just repeats the direction of expansion of the previous step (Figure 4a). In the case of the vertical/horizontal direction, the recursion is called for the expansion direction of the previous step and its two adjacent diagonal directions (Figure 4b). The situation after one step of the algorithm for all internal vertices neighboring $\vec{v_c}$ is shown in Figure 4c.

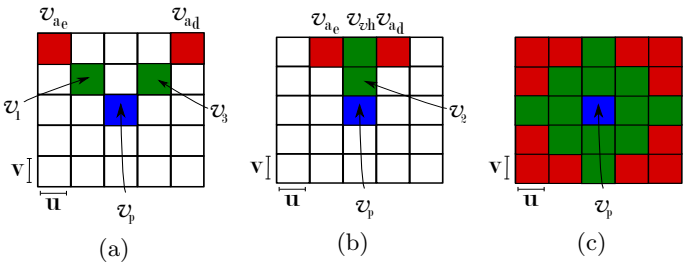

Fig. 4. Diagonal expansion example (a) and vertical/horizontal example (b). A single algorithm pass, after all neighbors of $\overrightarrow{v_c}$ are calculated, is presented in (c).

Border Treatment. When a vertex $\vec{v_i} \in \mathbf{V}_{d_c}$ is at the border of the mesh, meaning it has coordinates $u = \{0 \text{ or } m_u\}$ and/or $v = \{0 \text{ or } m_v\}$, the method needs to modify its routine to promote expansion. If the vertex coordinate reaches $u = 0$ the next step of the algorithm will map this coordinate to $u = m_u - 1$ and, similarly, if the coordinate is $u = m_u$ the next step of the algorithm will map this coordinate to $u = 1$. In the case of the v coordinate (latitude), if a vertex reaches a border coordinate, the algorithm simply stops propagating.

The leap of one coordinate for the longitude case is deliberate, reflecting that for coordinates $u = 0$ and $u = m_u$ there is an overlap. If a vertex has a border coordinate u on the terrain, any change made in the heightmap and error maps for this vertex must be repeated at the other end of the heightmap to prevent cracks on the terrain. An example of border treatment can be seen in Figure 5.

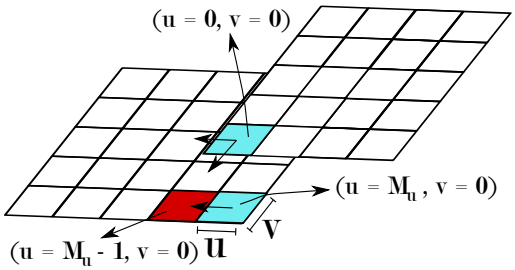

Fig. 5. Border treatment in the case of vertices trying to expand beyond the dimensions of the terrain. For the latitude, if a vertex $\vec{v}$ goes beyond the dimensions of the terrain, the expansion is interrupted in that direction. In the case of longitude, the coordinate of the vertex u is modified so that it can continue expanding.

6.4 Error and Height Propagation

Determined the area of deformation, or set $\mathbf{V}_d \in \mathbf{V}$, it is necessary to propagate error and height values for all vertices in the set $\mathbf{V}_d$. The propagation algorithm can be defined as an extension of the area determination algorithm, since both run through all vertices that have the property $I(u, v)$.

Height Definition and Propagation. The function used in this paper to calculate the height values is the Gaussian distribution function $g(x)$ described by Equation 7. The function has a maximum at the control vertex and a minimum at the border of the area of deformation. In this function, the standard deviation is σ and the average is μ.

$$g(x) = \frac{1}{\sigma\sqrt{2\pi}} e^{-\frac{(x-\mu)^2}{2\sigma^2}}. \tag{7}$$

The process involves a mapping from the discrete to the continuous domain and vice versa. A vertex $\vec{v} \in \mathbf{V}$ is mapped on the sphere and tested to see whether it is or not within the area of deformation. If it is an internal vertex, the Euclidean distance in $\mathbb{R}^3$ of the vertex $\vec{\mathbf{v}}$, mapped by f, to the control vertex $\vec{\mathbf{v_c}}$, is passed to the Gaussian function defined by Equation 7 and a height value is obtained. This value is then associated with a scalar w and stored in the heightmap at its coordinates (u, v). The new value of w is accessed on the next tessellation step, where the mapping function will transmit the modification made on the heightmap to the surface of the terrain.

Metric and Error Propagation In the same way as the propagation of height values, it is desired to cover all vertices $\vec{v} \in \mathbf{V}_d$ for the error propagation. One restriction to be recalled is that the error metric must preserve the monotonicity, meaning that the parents have higher error value than their children.

To propagate error in the correct way, it is necessary to use an expansion function that traverse the mesh in a hierarchical manner. This is possible using the concept of alternate step. Consider a number of iterations $i = 0, 1, 2, ..., n$ and a step size p_a. Knowing that every leaf node in the triangle bintree has error $\varepsilon_T = 0$ and that the error grows as we reduce the resolution level until the root node is reached, it is possible to notice in the tree that the position of the nodes is spaced in a homogeneous way for similar error values.

Consider, for instance, Figure 6a that shows the displacement of the vertices that have error $\varepsilon_T = 0$ in a triangle in the highest level of resolution. It is possible to notice that one can walk on the structure covering all vertices in this resolution, using steps p_l of odd steps in the vertical direction, followed by "walks" in both diagonal directions of the vertex reached by an initial step.

In a more specific way it is possible to state in this case, that the initial step of each iteration i is given by Equation 8 and the step increment i_c is given by Equation 9. In this case where the resolution is maximum, the iteration is $i = 0$,

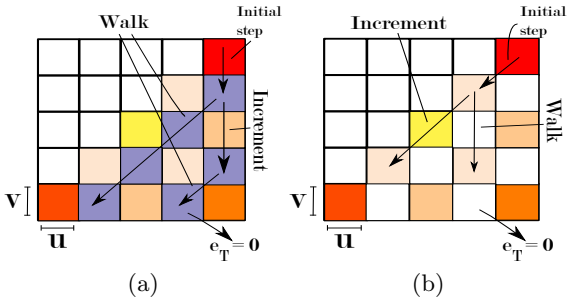

Fig. 6. Hierarchical expansion example. In (a) the first case occurs, vertical step and diagonal walk. In (b) the second case happens, diagonal step and vertical walk, both on the zero value iteration.

the initial step $p_l = 1$, the step increment $i_c = 2$ in the vertical direction and the step for the diagonal walk $p_d = p_l$.

$$p_l = 2^i. \tag{8}$$

$$i_c = 2 * p_l. \tag{9}$$

To the level immediately below the maximum, the model modifies itself (Fig. 6b). The initial step and the increment are obtained in the same way as in the previous case, following Equations 8 and 9. The iteration is again $i = 0$, $p_l = 1$ and $i_c = 2$. In this case, although, the initial step is done in the diagonal direction and the walk through the structure is done in the vertical direction (the inverse of the previous case). The recursion walks vertically with a step $p_a = i_c$, being $p_a = 2$ for this resolution.

The combination of these cases allows that all vertices are traversed. An algorithm can be easily extracted from these two cases, representing a hierarchical manner to cover the A4-8 mesh. The monotonicity is guaranteed this way, because the error can still be calculated with a bottom-up approach.

7 Results

All experiments were done on a computer with an AMD FX(tm)-6100 six cores processor, 8GB RAM and GeForce GTX 550 Ti with 2GB of RAM. The Microsoft LifeCam camera was used as video capture device. A resolution of 640×480 *pixels* was defined for all visualization windows. In order to validate the method, meshes with maximum resolution of 2049×2049 and 8193×8193 vertices were chosen. The maximum number of triangles generated by the tesselation process was defined as 70000.

As the user modifies the distance from the terrain to the camera, the view-dependent error changes, and the mesh adapts itself through refinement or simplification. Figure 7 shows an example of mesh change due to terrain scale modification. The initial position of the terrain can be seen in Figure 7b, mesh

modifications when the camera approaches the terrain is seen in Figure 7c and when it moves away in Figure 7a.

(a) (b) (c)

Fig. 7. Mesh modifications related to the distance between the camera and the terrain. Terrain initial position (b), camera close to the terrain (c) and moved away from it (a).

The deformation of a spherical terrain with the proposed method can be seen in Figure 8. The image shows a sequence of frames, from left to right, where the user performs a movement with the marker through the terrain surface causing deformation.

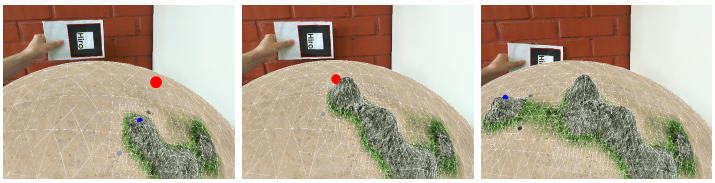

Fig. 8. A sequence of frames spaced in time showing the mesh being deformed using the proposed method.

Here, the maximum image error $dist_{max}$ tested varied from 0.1 to 6.0. Experiments shown that the ideal value, that promote balance between visualization quality and number of triangles, is $dist_{max} = 4.0$.

The radius of deformation r_d used during testing ranged from 150km to 600km, being the radius of the spherical terrain equal to 6372.79km. In all experiments, the area of deformation change in the $\mathbb{R}^3$ space for three different radius of deformation defined as: 150km, 300km and 600km

The average time that the application takes to render one frame with the terrain being deformed was calculated for different resolutions. The camera was fixed in a single position for all values contained in Tables 1 and 2. The chosen position was kept at a distance of three times the radius of the sphere to its center, being approximately $19,000$km.

In the case of deformation, the worst case scenario was chosen to evaluate the method. In other words, the longitude was set at 180°, where the vertices have coordinates $u = 0$ and $u = m_u$ for variables values of latitude. Latitude

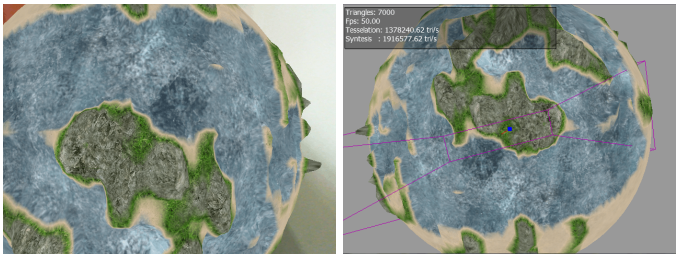

(a) (b)

Fig. 9. Final terrain visualization generated with the proposed method. Global scale (a) and local scale (b).

values begin at 0° and increase 30° until they reach 180°, in other words, from one pole to the other. The average time to render a frame without deformation being applied to the terrain was 0.033 seconds.

The values in Table 1 represent the average time to render a frame with the terrain being deformed for a maximum resolution of 2049×2049 vertices. It is possible to affirm that, for a radius of deformation $r_d = 150$km, any region of the planet may be deformed without the user noticing drops in the number of frames per second. For a radius of $r_d = 600$km, the application takes three times longer to render a frame with deformation occurring at the pole than at the equator, but the number of vertices deformed at the pole is about 90 times greater when compared to the equator region.

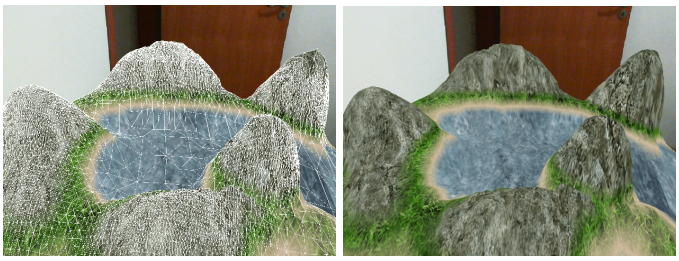

(a) (b)

Fig. 10. A complete deformation scenario. Terrain with edges drawn (a) and without (b).

Table 2 lists values for the higher terrain resolution tested, 8193×8193 vertices. For a deformation radius of $r_d = 600$km, one realizes that the average time start to rise for all tested latitudes. This means that, as the resolution increases, it is necessary to reduce the deformation radius in order to exchange application performance and display quality.

Latitude	Average time(s)			Latitude	Modified Vertices		
0	0.064	0.096	0.117	0	32764	63471	126700
30	0.041	0.047	0.051	30	698	2789	11467
60	0.041	0.047	0.044	60	397	1593	6650
90	0.041	0.046	0.043	90	360	1431	5737
120	0.038	0.044	0.050	120	405	1629	6560
150	0.045	0.047	0.050	150	704	2916	11543
180	0.063	0.086	0.116	180	32759	63463	126888
	$r_d = 150$km	$r_d = 300$km	$r_d = 600$km				

Table 1. Average rendering time of the terrain in seconds when a number of vertices are modified at a certain latitude. Maximum resolution of 2049×2049 vertices.

Latitude	Average time(s)			Latitude	Modified vertices		
0	0.356	0.711	1.328	0	507744	1006861	2013967
30	0.052	0.053	0.114	30	11302	45437	180019
60	0.045	0.052	0.098	60	6532	25752	106635
90	0.035	0.047	0.082	90	5765	23056	89330
120	0.046	0.051	0.083	120	6511	26024	101521
150	0.045	0.059	0.107	150	11329	45625	179929
180	0.350	0.720	1.333	180	507805	1007216	2013721
	$r_d = 150$km	$r_d = 300$km	$r_d = 600$km				

Table 2. Average rendering time of the terrain in seconds when a number of vertices are modified at a certain latitude. Maximum Resolution 8193×8193 vertices.

A complete deformation scenario can be seen in Figure 10. A planet generated with the proposed method is shown in Figure 9. The implementation of the proposed method can cope with deformations in real time even if the speed of rotation of the planet is set to a high value. It is important to note that adaptive meshes are usually used only for visualization, here the final application can both visualize and modify a terrain in real time.

8 Conclusion

Interactive systems providing real 3D modeling freedom are rare. In this work, we propose an interactive method for 3D modeling of spherical terrains in real time through augmented reality. The entire process is easy to be controlled by the user. Nevertheless, the generated terrain can be quite complex, natural-looking, even if defined by a small number of user actions.

The proposed method proved to be efficient in dealing with different resolutions. The increase of the average rendering time is lower than the increase in the number of modified vertices for all tests. The hierarchical propagation allows that all vertices in an area of deformation are visited, complying with the monotonicity constraint of the error metric.

The use of a physical marker to deform a mesh, provides an intuitive interface to create shapes and patterns across the terrain. This interface allows easy

surface modeling and manipulation, without requiring prior knowledge in 3D modeling softwares such as *Maia* and *3D Studio*.

The combination of known techniques with the A4-8 mesh structure produced the desired results, it is possible to not only generate a terrain with a few movements, but also add detail at any resolution. Although the visualization and modeling steps are done sequentially, the application runs in real time for various resolutions. This means that a large but highly detailed terrain can be generated with the proposed method.

References

1. Coquillart, S.: Extended free-form deformation: a sculpturing tool for 3d geometric modeling. In: Proceedings of the 17th annual conference on Computer graphics and interactive techniques. SIGGRAPH '90, New York, NY, USA, ACM (1990) 187–196
2. Singh, K., Fiume, E.: Wires: A geometric deformation technique (1998)
3. Sumner, R.W., Schmid, J., Pauly, M.: Embedded deformation for shape manipulation. ACM Trans. Graph **26** (2007) 80
4. Kobbelt, L.P., Bareuther, T., peter Seidel, H.: Multiresolution shape deformations for meshes with dynamic vertex connectivity (2000)
5. Sha, C., Liu, B., Ma, Z., Zhang, H.: Multi-resolution meshes deformation based on pyramid coordinates. In: CGIV, IEEE Computer Society (2007) 200–204
6. Velho, L., Gomes, J.: Variable resolution 4-k meshes: Concepts and applications. Comput. Graph. Forum **19**(4) (2000) 195–212
7. Kato, H., Billinghurst, M.: Marker tracking and hmd calibration for a video-based augmented reality conferencing system. In: Augmented Reality, 1999. (IWAR '99) Proceedings. 2nd IEEE and ACM International Workshop on. (1999) 85 –94
8. Nealen, A., Mueller, M., Keiser, R., Boxerman, E., Carlson, M.: Physically Based Deformable Models in Computer Graphics. Computer Graphics Forum **25**(4) (December 2006) 809–836
9. Baraff, D., Witkin, A.: Large steps in cloth simulation. In: Proceedings of the 25th annual conference on Computer graphics and interactive techniques. SIGGRAPH '98, New York, NY, USA, ACM (1998) 43–54
10. O'Brien, J.F., Hodgins, J.K.: Graphical modeling and animation of brittle fracture. In: Proceedings of the 26th annual conference on Computer graphics and interactive techniques. SIGGRAPH '99, New York, NY, USA, ACM Press/Addison-Wesley Publishing Co. (1999) 137–146
11. Gregory, A.D., Ehmann, S.A., Lin, M.C.: intouch: Interactive multiresolution modeling and 3d painting with a haptic interface. In: Proc. of IEEE VR Conference. (1999) 45–52
12. Do, T.V., Lee, J.w.: 3darmodeler : a 3d modeling system in augmented reality environment. Systems Engineering **4** (2010) 2
13. Duchaineau, M.A., Wolinsky, M., Sigeti, D.E., Miller, M.C., Aldrich, C., Mineev-Weinstein, M.B.: Roaming terrain: real-time optimally adapting meshes. In: IEEE Visualization. (1997) 81–88
14. Stockman, G., Shapiro, L.G.: Computer Vision. 1st edn. Prentice Hall PTR, Upper Saddle River, NJ, USA (2001)